Chapter 16
Structural Design with Joints for Maximum Dissipation

M. Stender, A. Papangelo, M. Allen, M. Brake, C. Schwingshackl, and M. Tiedemann

Abstract Many engineered structures are assembled using different kinds of joints such as bolted, riveted and clamped joints. Even if joints are often a small part of the overall structure, they can have a massive impact on its dynamics due to the introduction of nonlinearities. Thus, joints are considered a design liability. Significant effort has been spent in joint characterization and modelling, but a predictive joint model is still non-existent. To overcome these uncertainties and ensure certain safety standards, joints are usually overdesigned according to static considerations and their stiffness. Especially damping and nonlinearity are not considered during the design process. This can lead to lower performance, lower payload, and as result of the joints structural dynamic models often do a poor job of predicting the dynamic response. However, it is well-known that, particularly for metal structures, joints represent the main source of energy dissipation. In this work a minimal model is used to show how structural performance can be improved using joints as a design variable. Common optimization tools are applied to a nonlinear joint model in order to damp undesired structural vibrations. Results illustrate how the intentional choice of joint parameters and locations can effectively reduce vibration level for a given operating point of a jointed structure.

Keywords Joints • Dissipation • Optimization • Design • Nonlinear dynamics

16.1 Introduction

Many structures from automotive, aerospace and civil engineering are assembled by joints such as bolted, riveted and clamped joints. These joints introduce nonlinear dynamical behavior and uncertainties [1–3] even if they are just a small part of the overall structure. Also, joints are one of the main sources of energy dissipation in metal structures [2, 3, 4]. During the design process of engineering structures, maximum stress levels and vibration amplitudes during operation are calculated using mathematical models. As joints can strongly affect the dynamic behavior, they have to be included in the mathematical model. A great effort has been spent in the characterization of joints, but reliable and predictive models are still non-existent. Therefore, joints are considered rather a design liability than a design parameter. Because joints are not considered in the design, non-optimal designs are achieved, which have large vibration amplitudes or are heavier than needed.

Various studies have considered the problem of finding the optimal linear damping and stiffness parameters which minimize the vibration level of an undamped linear structure with one [5] or more [6] degrees of freedom, while this work focuses on a nonlinear model of the joint, i.e. the Jenkins model. The ultimate goal of this paper is to demonstrate

M. Stender (✉)
Dynamics Group, Hamburg University of Technology, Schlossmuehlendamm 30, 21073 Hamburg, Germany
e-mail: merten.stender@tuhh.de

A. Papangelo
Department of Mechanics Mathematics and Management, Polytechnic of Bari, Viale Japigia 182, 70126 Bari, Italy

M. Allen
Department of Engineering Physics, University of Wisconsin, 1500 Engineering Drive, Madison, WI 53706, USA

M. Brake
Component Science and Mechanics, Sandia National Laboratories, MS 1070, Albuquerque, NM 87185-1070, USA

C. Schwingshackl
Imperial College London, Exhibition Road, SW7 2AZ London, UK

M. Tiedemann
Dynamics Group, Hamburg University of Technology, Schlossmuehlendamm 30, 21073 Hamburg, Germany

Audi AG, 85057 Ingolstadt, Germany

A. Brandt, R. Singhal (eds.), *Shock & Vibration, Aircraft/Aerospace, Energy Harvesting, Acoustics & Optics, Volume 9*,
Conference Proceedings of the Society for Experimental Mechanics Series, DOI 10.1007/978-3-319-30087-0_16

the performance improvement that might be achieved by exploiting joints, hopefully motivating the development of improved testing, modeling and design methods that consider the joints. A minimal model is studied and the joint model is considered to be predictive so that changes to the joint parameters (e.g. the clamping pressure) can be related to the response. While the simple model used here may not prove to be predictive in many real scenarios, it does provide a useful test case that captures some important physics. The structural response is numerically computed and optimization routines are adopted to show how it can be improved by the intentional choice of joint parameters. In particular the idea behind is to design not only the structure but also the joint to be able to damp vibrations in frequency ranges of interest. By minimizing the peak displacements in the simple model, the peak stresses in the structure would presumably decrease and the fatigue life would be improved, reducing wear and maintenance costs. We discuss different joint locations to show advantages and disadvantages of these choices which can help the designer during the design process.

16.2 The Model

This work employs a four degree of freedom (4-DOF) model including a nonlinear joint as depicted in Fig. 16.1. The structure consists of four masses m which are assembled by springs of stiffnesses k. The harmonic external forcing $F_{\text{ext}} = A\cos(2\pi f_{\text{ext}} t)$ acts on the first mass. In order to be able to compare Frequency Response Functions (FRF), constant modal damping ξ is applied to every mode [7]. The joint is represented by a Jenkins model. The joint's effect on the system response will be studied in two different positions: (a) joint located between the second and third mass, and (b) joint located between the third mass and the ground. These positions represent the fundamental locations of joints in engineering structures—either assembling two moving substructures or clamping a structure to a rigid body.

The LuGre formulation [5] is employed for the definition and implementation of the joint model, see Eq. (16.1). The tangential joint stiffness is denoted by k_{t} and the normal load by N. Therefore in the limit of full sliding and full stick, the sliding force is described by $\mu_{\text{k}}N$, whereas the sticking force is f_{S}. The transition from the sticking to the sliding state is described by an exponential decay depending on the Stribeck velocity v_{s} and the relative joint velocity $\dot{u} = \frac{du}{dt}$, where u is the relative displacement experienced by the joint. During the numerical simulation the differential Eq. (16.1b) is solved and the joint force f_{LuGre} computed.

$$g(\dot{u}) = \mu_{\text{k}}N = (f_s - \mu_{\text{k}}N)e^{-\left(\dot{u}/v_s\right)^2} \tag{16.1a}$$

$$\dot{q} = \dot{u} - \frac{k_{\text{t}}|\dot{u}|}{g(\dot{u})}q \tag{16.1b}$$

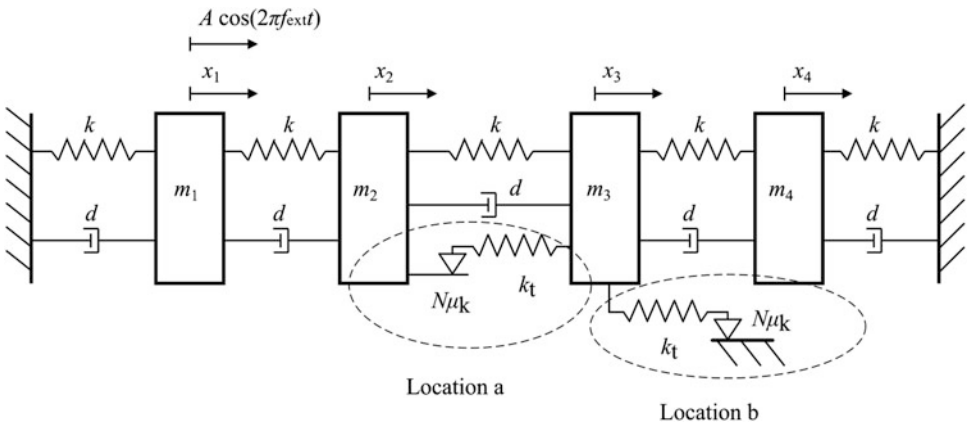

Fig. 16.1 4-DOF system with Jenkins element and joint locations discussed in this work

$$f_{\mathrm{LuGre}}(\dot{u}) = k_{\mathrm{t}} q \tag{16.1c}$$

The default model parameters read $m_{1,\ldots,4} = 1\,\mathrm{kg}$, $k = 40,000\,\mathrm{N/m}$, $\xi = 0.001$, $A = 0.1\,\mathrm{N}$, $k_{\mathrm{t}} = 40,000\,\mathrm{N/m}$, $\mu_{\mathrm{k}} = 1$, $N = 1\,\mathrm{N}$, $f_{\mathrm{s}} = 5\,\mathrm{N} + N$ and $\nu_{\mathrm{s}} = 5 \cdot 10^{-4}\mathrm{m/s}$.

16.3 The Method

To compute the response of the structure, the nonlinear frequency response function of each mass has to be determined. Appropriate cost functions are defined and evaluated to obtain a scalar value ('cost value') which at each frequency is representative of the structural dynamic response. The resulting cost value is finally subject to the optimization routine. Hereafter, these key methods are introduced.

16.3.1 Numerical Continuation Method

The numerical continuation toolbox MATCONT [8] is utilized to compute frequency response functions of the system. It employs orthogonal collocation methods which discretize a (partial) differential equation at collocation points. Initialized with stable attractors of the system, such as equilibrium points or limit cycles, a solution curve can be approximated. The solution found previously can then be tracked in the direction of the continuation parameter using predictor-corrector steps. The continuation is initialized at a low value of the excitation frequency. In order to obtain the frequency response function, a continuation of the nonlinear solution is performed for the continuation parameter f_{ext}.

16.3.2 Merging of Frequency Response Functions

For the 4-DOF model the displacement x_i of every mass i is available for investigation. Dividing each displacement x_i by the excitation amplitude A yields four receptances R_i [m/N]. As the structural performance of the whole structure will be subject to an optimization, a scalar cost value is required to represent the vibration level. Thus, either the receptance of a single mass has to be selected as base for the scalar cost value, or the four receptances have to be merged into one combined receptance. In order to capture the overall system behavior a combined receptance $\overline{R}$ is used for this work. Therefore, the maximum receptance for every frequency point j is selected to compose a single data set $\overline{R}$ that represents the vibration level of the structure. The use of the maximum value ensures to consider the maximum displacement amplitude and thus the maximum stresses the structure undergoes.

$$\overline{R}(R_i) = \max_{\substack{i = 1,\cdots,4 \\ j = 1,\cdots,n_{\mathrm{f}}}} \left(R_i^j\right) \in [f_{\mathrm{l}}, f_{\mathrm{u}}] \tag{16.2}$$

In Eq. (16.2) $[f_{\mathrm{l}}, f_{\mathrm{u}}]$ is the frequency interval chosen and n_f the number of frequency points considered on the interval.

16.3.3 Cost Function

The objective of the optimization is to reduce vibration amplitudes in a certain frequency range. Therefore, an appropriate cost function based on the merged receptance $\overline{R}$ needs to be defined. Typically, frequency ranges in the vicinity of resonance frequencies are considered critical in practical applications. Hereafter, the peak value of the merged receptances within the frequency range $[f_{\mathrm{l}}, f_{\mathrm{u}}]$ is defined as the scalar cost value:

$$\Psi = R_{\text{peak}} \in [f_{\text{l}}, f_{\text{u}}] \tag{16.3}$$

16.3.4 Optimization Algorithm

The optimization is carried out by the MATLAB built-in method 'fmincon' which can perform bounded, nonlinearly constrained optimizations. This method is based on the sequential quadratic programming (sqp) algorithm [9], which iteratively solves a sequence of subproblems using a quadratic model of the objective. If no constraints are applied this method reduces to Newton's algorithm finding a point with zero gradient of the objective. The free joint parameters $\mathbf{p}$ serve as input values and the cost value Ψ as objective for the minimization giving the optimal parameter configuration $\hat{\mathbf{p}}$.

$$\hat{\mathbf{p}} = \min_{\mathbf{p}} (\Psi(\mathbf{p})) \in [\mathbf{p}_{\min}, \mathbf{p}_{\max}] \tag{16.4}$$

The termination tolerance on the parameter is chosen to be $tolX = 10^{-4}$ and the termination tolerance on the cost function value $tolFun = 10^{-6}$.

16.4 First Model Studies

The joint parameters k_{t} and N (see Fig. 16.1) are used as free parameters during the optimization process while all structure parameters are kept fixed. First, the qualitative influence of both joint parameters are discussed. The friction coefficient μ_{k} is kept constant so that the normal load N controls the sliding or sticking behavior of the joint for a given joint force. The limiting cases of very small and very large normal loads linearize the system. The joint becomes inactive for normal loads tending to zero as it always slides without dissipating. Large normal loads compared to the excitation amplitude result in a stuck joint adding the linear stiffness k_{t} to the system. The tangential stiffness affects the dominance of the joint and thus the impact the joint has on the structure: for small values of k_{t} compared to k, the joint becomes inactive and the system behaves linearly. Thus, the parallel connected stiffnesses k and k_{t} and the normal load N control the sliding state of the joint for a given excitation amplitude. This observation implies the introduction of two dimensionless parameters α and β.

$$\alpha = \frac{k_{\text{t}}}{k} \quad \beta = \frac{N}{A} \tag{16.5}$$

As the considered model is nonlinear, it is important to first verify that the two dimensionless parameters that were chosen remain valid. To check this, the frequency response functions were compared for different values of the dimensional parameters—once keeping the structure parameter (k, A, respectively) fixed, once keeping the joint parameter (k_{t}, N, respectively) fixed for the same dimensionless parameters. The results of this verification step are not shown here, but they did show perfect agreement of the frequency response functions: for a given value of the dimensionless parameter the system response is the same regardless of the choice of the dimensional parameters (either joint or a structure parameters). Hence, the system is completely defined by the two dimensionless parameters α and β which are therefore valid for further investigations. This result meets the experience from different fields of joint research: the force ratio β is a well-known parameter in the analysis of underplatform dampers [4, 6]. For the default configuration the parameters are chosen to be $\alpha = 1$ and $\beta = 1$.

Figures 16.2 and 16.3 depict the impact of the stiffness ratio α and the force ratio β on the system dynamics. Generally, stiffness is added to the structure when α is larger than 1. Consequently, the resonance frequencies rise and resonance amplitudes decrease as shown in Fig. 16.2. The study of different values of the force ratio β reveals the linearizing effect of the limiting cases $\beta \to 0$ (purely sliding joint) and $\beta \to \infty$ (completely stuck joint). The choice of a particular force ratio drives the system to a state within those linear limits. For this particular joint location (a), only the second and fourth modes are affected by the joint since only these modes exhibit out of phase movement of masses m_2 and m_3. If the joint is instead attached to the ground (joint location (b)) all modes are affected. Already at this stage it is clear that the intentional choice of the joint parameters has a strong influence on the system dynamics and the vibration levels that the structure experiences.

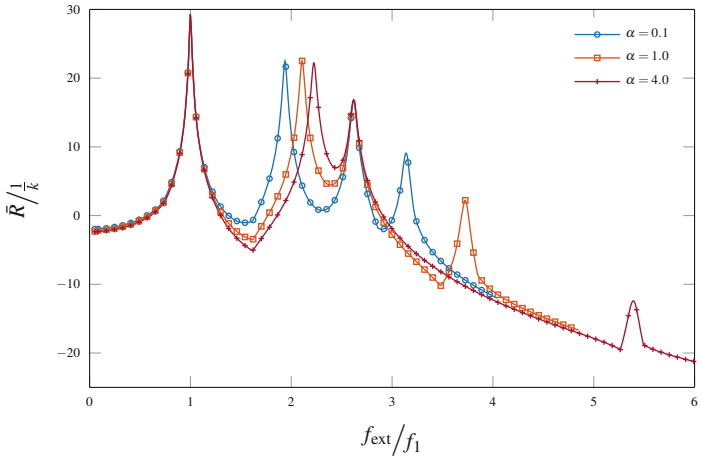

Fig. 16.2 Impact of stiffness ratio ($\alpha = 0.1$ [*circles*], $\alpha = 1.0$ [*squares*], $\alpha = 4.0$ [*crosses*]) on dynamic behavior of the default system configuration for fixed force ratio $\beta = 10$ and joint location (a)

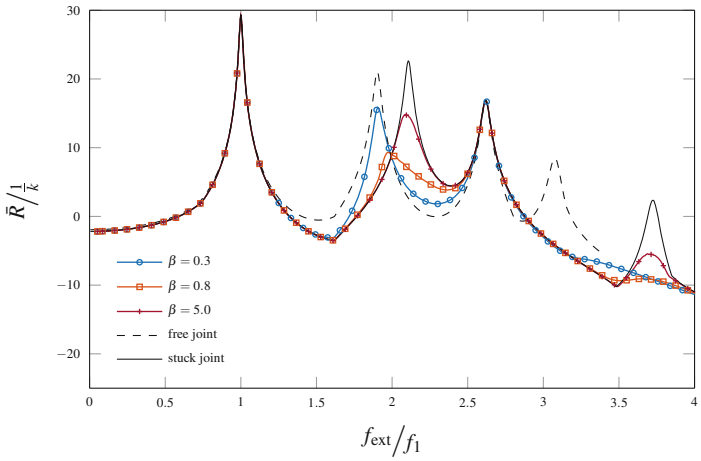

Fig. 16.3 Impact of force ratio ($\beta = 0.3$ [*circles*], $\beta = 0.8$ [*squares*], $\beta = 5.0$ [*crosses*]) on dynamic behavior of the default system configuration for fixed stiffness ratio $\alpha = 1$ and joint location (a). The limiting linear cases are labeled by *dashed* (free) and *solid* (stuck joint) *black lines*

16.5 Joint Included in Structure

The first optimization case focuses on the joint location (a) (joint interposed between second and third masses). Both dimensionless parameters α and β are considered as free parameters. All structure parameters are kept constant and the second mode is selected to be the objective of the optimization. Hence, the amplitude of the merged receptances at the second mode is employed as the cost value. Starting from the initial parameter configuration $\mathbf{p}_0 = [\alpha, \beta]^{\mathrm{T}} = [0.4, 4.5]^{\mathrm{T}}$ an unconstrained but bounded optimization is performed.

After $i = 14$ iterations the optimization algorithm provides the optimal parameter configuration $\hat{\mathbf{p}} = [2.0, 0.74]^{\mathrm{T}}$. Figure 16.4 depicts the contour of the cost value on the selected optimization regime and the optimization path of the unconstrained optimization, drawn with white triangles. The starting point corresponds to low joint stiffness and high normal load values. Generally, the single Jenkins element dissipates the maximum energy for a distinct relative displacement. As only the force and stiffness ratios are subject to the optimization, the cost value reveals one global minimum on the parameter space, compare the concave characteristic of the cost value in Fig. 16.4.

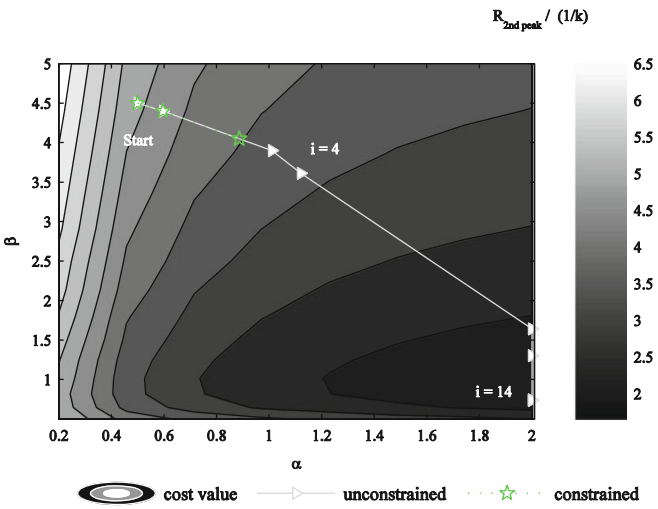

Fig. 16.4 Normalized vibration level of second mode and paths of unconstrained (*white*, *triangles*) and constrained (*green*, *stars*) optimization, for joint location (a)

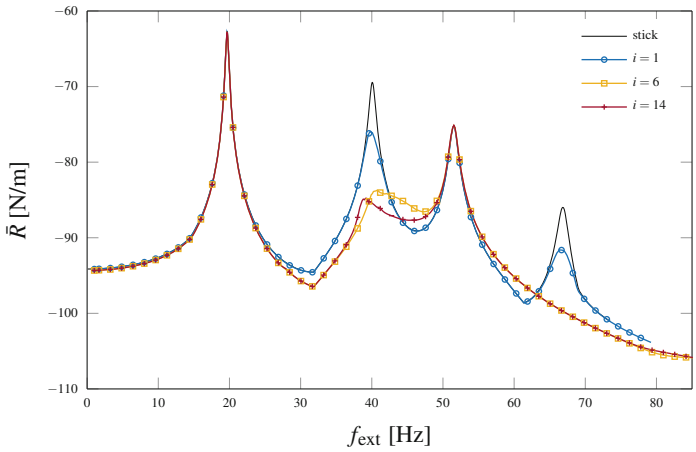

Fig. 16.5 Merged receptances $\overline{R}$ during optimization iterations $i = 1$ [*circles*], $i = 6$ [*squares*] and $i = 14$ [*crosses*] for joint location (a)

Figure 16.5 depicts the merged receptances for different optimization iterations i. Compared to the linear case of a stuck joint the vibration level of the second mode is reduced by 82.9 %. The reduction with respect to the nonlinear FRF of the initial configuration is 63.8 %. Only the second and fourth mode are affected by the joint since only these modes reveal out-of-phase motion with respect to mass m_2 and m_3. The optimization path from Fig. 16.4 can be divided into two main parts. First, the optimization algorithm mainly increases the joint stiffness value up to the maximum value allowed for the stiffness ratio ($\alpha = 2$) at iteration index $i = 6$. Then, the optimization heads in the direction of lower normal force on the Jenkins element to find the optimum. Physically, the deflection shapes are distorted by the increase of stiffness. Consequently, the energy feed-in is influenced (phase between vibration of mass m_1 and the forcing) as well as the energy dissipation (relative displacement of the joint). The first mechanism dominates the first part of the optimization path (increase of α) while the latter characterizes the second part (mainly decrease of β). Figures 16.6 and 16.7 emphasize these two generic concepts: During the first six optimization iterations the work put into the system is dramatically reduced while only a small decrease can be observed for iterations 7–14, compare Fig. 16.7. The corresponding hysteresis loops shrink during the first six iterations. Then, the maximization of dissipation takes place. This can be clearly seen from the growth of area enclosed by the hysteresis loops from iteration $i = 6$ to iteration $i = 14$, see Fig. 16.6.

Due to the added stiffness the fourth mode shifts by 10 Hz (8.8 %) during the optimization. In real application it typically is not possible to increase the stiffness of the joint so dramatically without incurring large weight penalties. Furthermore, increases to the frequencies of other modes may cause their response to increase leading to new vibration problems. Hence, constrained optimization was also pursued to seek a more realistic solution. In a second case study, the modes were not permitted to shift by more than 2 % and the vibration level of all modes must not increase during the optimization. The result

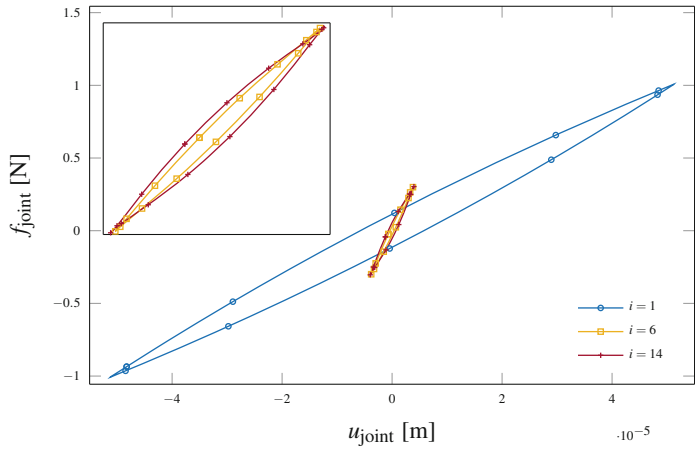

Fig. 16.6 Hysteresis loops and detailed view during optimization iterations $i = 1$ [*circles*], $i = 6$ [*squares*] and $i = 14$ [*crosses*] for the peak of 2nd mode, joint location (a)

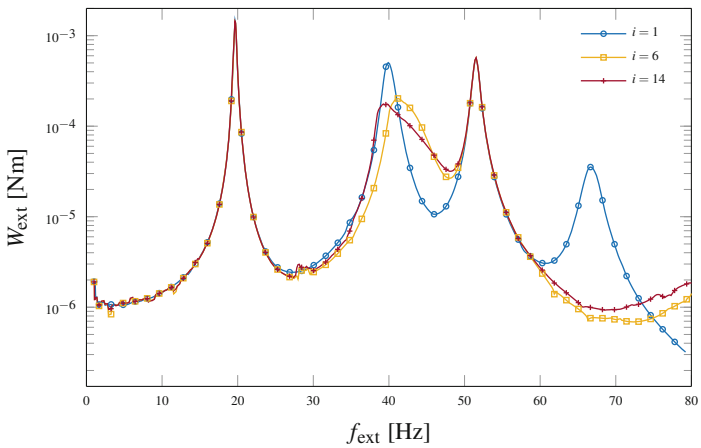

Fig. 16.7 Work put into the system by the external forcing during optimization iterations $i = 1$ [*circles*], $i = 6$ [*squares*] and $i = 14$ [*crosses*] for the peak of 2nd mode, joint location (a)

of the constrained optimization are depicted in Fig. 16.4 using green stars. Starting from the same point as the unconstrained optimization the direction of high joint stiffness is limited by the constraint on shifting modes. Therefore the optimization ends at a different optimal point with a 61.5 % reduction in the vibration level of the second mode, while simultaneously satisfying the constraints.

16.6 Joint Between Structure and Ground

The second case employs the joint location (b) (joint between third mass and ground). In this configuration the change of joint parameters affects every mode. Again, the optimization focuses on minimizing the response of the second mode which is started from the same point $\mathbf{p}_0$, in terms of joint parameters, as in the previous case for joint location (a). Figure 16.8 depicts the contour of the cost value for the 'ground' configuration (joint location (b)). In contrast to joint location (a) the

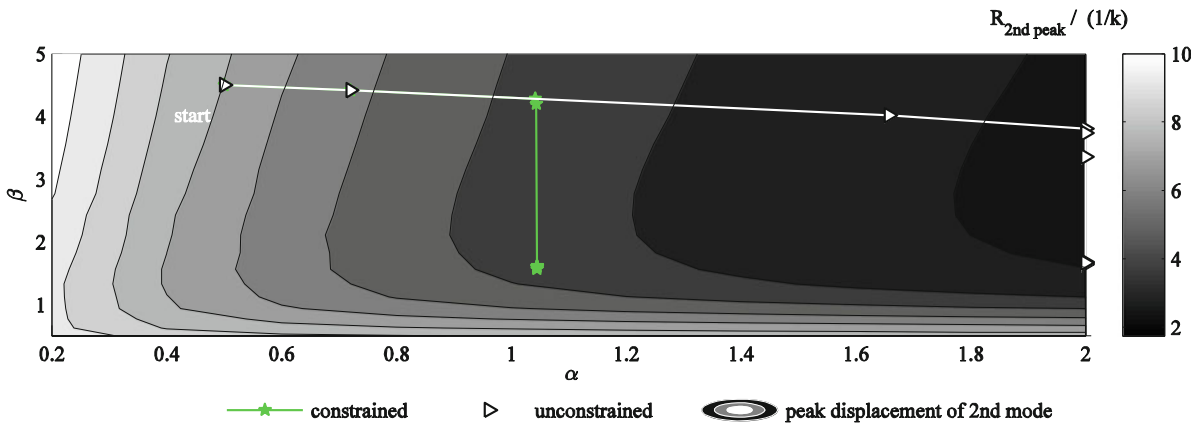

Fig. 16.8 Normalized vibration level of second mode and paths of unconstrained (*white*, *triangles*) and constrained (*green*, *stars*) optimization, joint location (b)

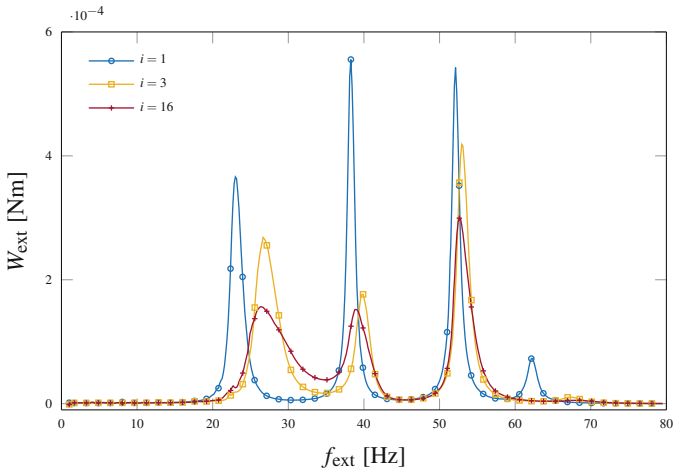

Fig. 16.9 Excitation work during optimization iterations $i = 1$ [*circles*], $i = 3$ [*squares*] and $i = 16$ [*crosses*], joint location (b)

cost value is much more sensitive to the stiffness ratio α than to the force ratio β. This observation is confirmed by the path of the unconstrained optimization. The optimization drives the system mainly to higher values of the joint stiffness. The reduction of the normal force does not affect the result as significantly. In this problem case, the optimization can generally take two different paths to minimize the vibration level of the structure: either maximize the dissipation in the joint or clamp the third mass to the ground via high values for the tangential stiffness. Here, the optimization pics the latter path. The introduction of a high stiffness between the structure and the ground physically represents a new constraint on the third mass which dramatically distorts the deflection shapes of the system. Thus, the minimization of vibration level is obtained by reduction of energy feed-in as already emphasized. Figure 16.9 illustrates the significant reduction of external work put into the system at the second mode. The reduction of vibration level of the second mode adds up to 77.3 % compared to the stick (linear) configuration, compare Fig. 16.10. In this case, a globally optimized system can be achieved since the vibration level of all modes decrease. This result illustrates the potential of intentional joint design in structural dynamics.

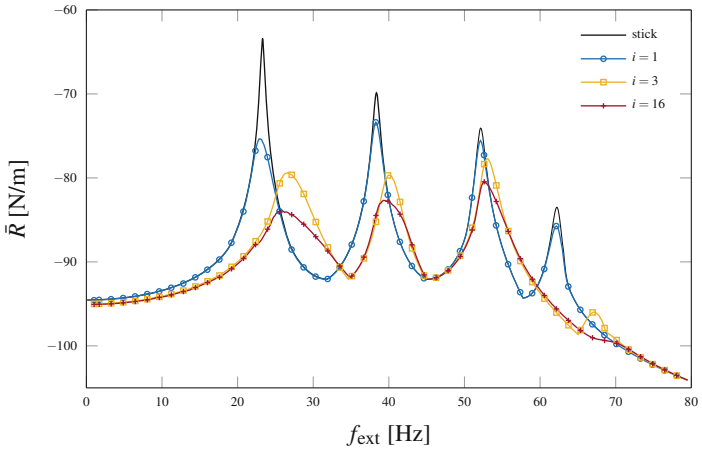

Fig. 16.10 Merged receptances during optimization iterations $i = 1$ [*circles*], $i = 3$ [*squares*], $i = 16$ [*crosses*] and the stick response [*solid black*], joint location (b)

16.7 Conclusion

This study on a minimal model shows how the structural performance of a given structure can be improved by joint design. For the studied model cases, the intentionally choice of joint parameters achieved vibration reductions of up to 82 % compared to the corresponding linearized joint stiffness model. In addition, different generic joint locations show different sensitivities to joint parameters. The main finding of this work is the twofold effect of joints on system dynamics: The optimization paths obtained can be clearly divided into two parts. Two different physical mechanisms, namely the reduction of energy feed-in and the increase of dissipation, are the root cause of this behavior. By varying the joint stiffness the deflection shapes are distorted. Therefore, the work put into the system is reduced and thus the vibration amplitudes decrease. In a second step, the optimization varies the normal load on the friction element to further decrease the vibration level by dissipation in the joint. In fact, the work dissipated in the joint is decreased in favor of higher joint stiffness to obtain the optimized solution. This result illustrates that when optimizing the response of a structure, it is important to consider both the damping and additional stiffness that joints introduce to the structure. The mutual reaction of the joint and the structure has to be accounted for. Despite the fact that a generic, oversimplified model is studied, these findings hopefully increase awareness of this interplay and are one step towards converting joints from design liabilities to design parameters which enable engineers to accomplish higher goals on reliability, wear and lightweight design than it is possible today. Further research is needed to develop accurate characterization and modeling for realistic joints, so this type of optimization can be performed on realistic structures.

References

1. Tiedemann, M., Kruse, S., Hoffmann, N.: Dominant damping effects in friction brake noise, vibration and harshness: the relevance of joints. Proc. Inst. Mech. Eng. D J. Automob. Eng. **229**(6), 728–734 (2015)
2. Padmanahban, K., Murty, A.: Damping in structural joints subjected to tangential loads. Proc. Inst. Mech. Eng. **205**, 121–129 (1991)
3. Padmanahban, K.: Prediction of damping in machined joints. Int. J. Mach. Tools Manuf. **32**, 305–312 (1992)
4. Sanliturk, K.Y., Ewins, D.J., Stanbridge, A.B.: Underplatform dampers for turbine blades: theoretical modelling, analysis and comparison with experimental data. Journal of Engineering for Gas Turbines and Power 123(4), 919–929 (2001)
5. Bograd, S., Reuss, P., Schmidt, A., Gaul, L., Mayer, M.: Modeling the dynamics of mechanical joints. Mech. Syst. Signal Process. **25**(8), 2801–2826 (2011)
6. Griffin, J.H.: Friction damping of resonant stresses in gas turbine engine airfoils. J. Eng. Gas Turbines Power **102**(2), 329–333 (1980)
7. Ewins, D.: Modal Testing: Theory, Practice, and Application, Mechanical Engineering Research Studies: Engineering Dynamics Series. Research Study Press (2000)
8. Dhooge, A., Govaerts, W., Kuznetsov, Y. A., Mestrom, W., Riet, A. M., & Sautois, B. : MATCONT and CL MATCONT: Continuation toolboxes in matlab. Universiteit Gent, Belgium and Utrecht University, The Netherlands (2006)
9. Nocedal, J., Wright, S.: Numerical Optimization, Springer Science & Business Media (2006)